

# Thermoanalytical study of the YSZ precursors prepared by aqueous sol–gel synthesis route

K. Tõnsuaadu · A. Zalga · A. Beganskiene ·  
A. Kareiva

CEEC-TAC1 Conference Special Issue  
© Akadémiai Kiadó, Budapest, Hungary 2012

**Abstract** The Y–Zr–O precursors derived from an aqueous sol–gel synthesis have been applied for the preparation of yttria-stabilized zirconia (YSZ) powders and thin films on the corundum ( $\text{Al}_2\text{O}_3$ ) substrate, using dip-coating technique. In this aqueous sol–gel synthesis route, citric acid as a complexing agent has been used for the preparation of stable Y–Zr–O nitrate–citrate sols and gels. Thermal decomposition of dried gels was studied by simultaneous TG/DTA/EGA-FTIR measurements in the dynamic 80%Ar + 20%O<sub>2</sub> atmosphere. FTIR and X-ray diffraction analyses were used for the determination of phase purity of the end products obtained at 700, 800 and 900 °C. The morphological features of the prepared YSZ coatings and powders were evaluated using scanning electron microscopy.

**Keywords** Sol–gel synthesis · TG/DTA/EGA-FTIR · Y–Zr–O nitrate–citrate complex

## Introduction

Yttria-stabilized zirconia (YSZ) is used as electrolyte for electrode-supported solid oxide fuel cells (SOFCs) due to their high ionic conductivity [1, 2]. The negligible electronic conductivity even under reducing atmosphere, the electrochemical stability as well as the mechanical properties of YSZ facilitate the use this material in fuel-cell

applications [3]. In order to increase the chemical stability of the SOFCs components and decrease the cell cost, it is necessary to decrease the working temperature to around 700–800 °C. The control of the microstructure and the thickness of the solid electrolyte may reduce the internal resistance of the YSZ electrolyte. Consequently, an improvement of the performance of the cell could then be reached [4–6]. Moreover, the synthesis of nanoscale materials, which could be used for the development of SOFC systems in the intermediate-temperature regime of 500 °C <  $T$  < 750 °C, now is of substantial interest [7].

The synthesis of YSZ powders and thin films on various substrates with a number of different techniques was previously published [8–15]. For this purpose, the solid-state, spray pyrolysis, non-aqueous sol–gel, hydrothermal methods, electrochemical, chemical vapour, physical vapour deposition, tape casting, slurry coating, and other techniques have been applied to synthesize bulk YSZ and dense ceramic coatings on different substrates for solid oxide fuel cells (SOFCs). All the coating techniques, mentioned before, have some advantages and disadvantages. However, the commercialization of SOFC on a big scale until today does not occur [16].

The technological applications of an aqueous sol–gel technique range in a very wide field, because of the versatility and simplicity of the method [17–19]. Compared with other techniques, an aqueous sol–gel method has the advantages of a good control of the processing parameters. The use of sol–gel processing can eliminate major problems such as long diffusion paths, impurities and agglomeration, which will result in products with improved homogeneity.

In this paper, we report on the synthesis and characterization of YSZ powders and thin films on the corundum substrates obtained using dip-coating technique. For the preparation of stable sols, an aqueous sol–gel synthesis

K. Tõnsuaadu (✉)  
Laboratory of Inorganic Materials, Tallinn University  
of Technology, Ehitajate tee 5, 19086 Tallinn, Estonia  
e-mail: kaia.tonsuaadu@ttu.ee

A. Zalga · A. Beganskiene · A. Kareiva  
Department of General and Inorganic Chemistry, Vilnius  
University, Naugarduko 24, 03225 Vilnius, Lithuania

approach in which citric acid as a complexing agent was used. The impact of a concentration of starting chemicals used in gel preparation, gels thermal behaviour including the analysis of the evolved gases by FTIR spectroscopy, phase purity and crystallinity of the annealed samples is studied.

## Experimental details

### Sample preparation

The Y-Zr-O nitrate–citrate sol was prepared by an aqueous synthesis route. In this case, the appropriate amount of zirconium oxonitrate dihydrate ( $\text{ZrO}(\text{NO}_3)_2 \cdot 2\text{H}_2\text{O}$ , 99.9%) was first dissolved in concentrated nitric acid solution (65%  $\text{HNO}_3$ ) by stirring at 70–80 °C. Three samples with different starting concentration of zirconium were prepared. The amount of  $\text{ZrO}(\text{NO}_3)_2 \cdot 2\text{H}_2\text{O}$  selected was 0.0025 mol (sample 1), 0.005 mol (sample 2) and 0.01 mol (sample 3). Secondly, citric acid (CA) with a molar ratio of  $\text{Zr}/\text{CA} = 0.25$ , dissolved in a small amount of distilled water, was added with a continuous stirring at the same temperature. Next, after 5 h, the required amount of yttrium nitrate hexahydrate ( $\text{Y}(\text{NO}_3)_3 \cdot 6\text{H}_2\text{O}$ , 99.99%) dissolved in distilled water, was mixed with the previous solution. Finally, the same amount of the aqueous solution of the complexing agent CA was repeatedly added to the reaction mixture in order to prevent crystallization of metal salts during the gelation process. The beaker with the solution was closed with a watch glass and left for 1 h with continuous stirring. The obtained clear solution was concentrated by slow evaporation at 80 °C in an open beaker. A pale yellow, transparent, Y-Zr-O nitrate–citrate sol formed after nearly 60% of the water has been evaporated under continuous stirring. The synthesis scheme is shown in Fig. 1.

Y-Zr-O nitrate–citrate gel was prepared by continuous stirring of the stable Y-Zr-O nitrate–citrate sol in an open beaker. After the evaporation of residual solvent at the same 70–80 °C temperature, the porous brown Y-Zr-O gel was formed. The obtained gel was repeatedly dried in an oven at 110 °C temperature, and fine-grained powders were obtained.

The Y-Zr-O precursor gels were calcined for 5 h at 500 °C in alumina crucibles and reground carefully in an agate mortar. Since the gels are very combustible, slow heating (1 °C/min), especially between 150 and 300 °C, was found to be essential. After intermediate grinding, the obtained powders were repeatedly annealed for 5 h at 700, 800 and 900 °C temperatures in air at ambient pressure.

YSZ thin films were deposited onto commercial corundum ( $\text{Al}_2\text{O}_3$ ; 1.5 × 1.5 cm) substrates by dip-coating technique from the stable Y-Zr-O nitrate–citrate sol. The films on corundum substrate were deposited at 5 mm/min

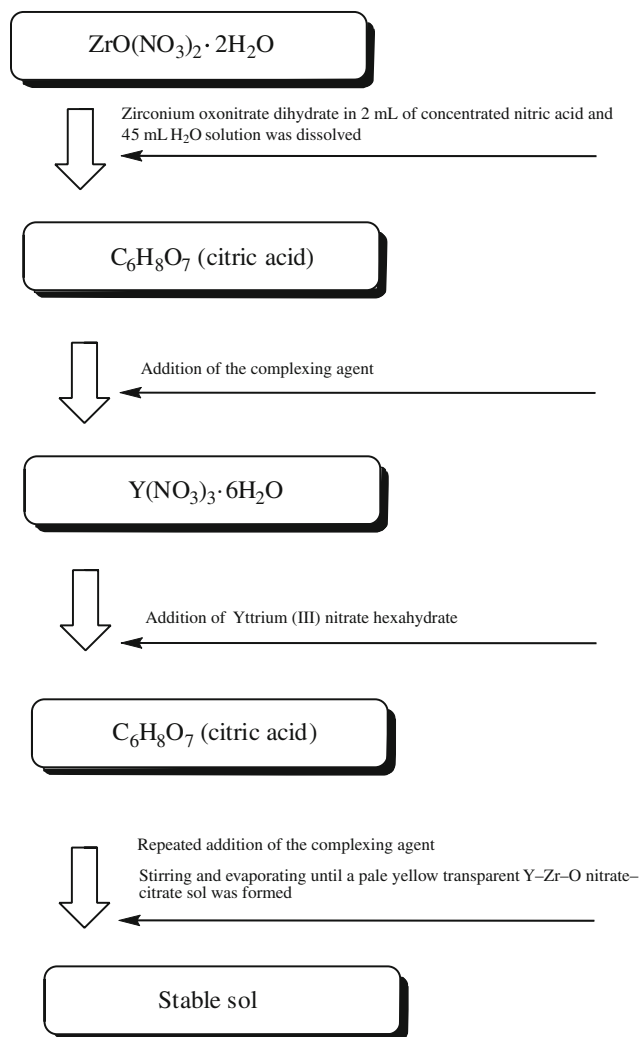


**Fig. 1** Synthesis scheme of the sol–gel preparation of the Zr–Y–O nitrate–citrate sol

immersion rate and were dried at room temperature for 24 h in air at ambient pressure in a horizontal position. Afterwards, the dried coated substrate was annealed at 800 °C temperature in air for 1 h. According to the previous studies [20, 21] at this temperature, the crystallization process begins, and a pure cubic phase of yttria-stabilized zirconia was obtained from the YSZ sol–gel film.

### Characterization of samples

The thermal decomposition processes of Y-Zr-O precursor nitrate–citrate gels were examined by thermogravimetric and differential thermal analysis (TG/DTA) combined with Fourier-transform infrared spectroscopy coupled with the evolved gas analysis (FTIR/EGA). The measurements were taken on a SetSys-Evolution instrument connected to a Nicolet 380 FTIR spectrometer using a sample weight of about 10–12 mg in open Pt crucibles and a heating rate of

10 °C min<sup>-1</sup> in flowing artificial (80%Ar + 20%O<sub>2</sub>) air (60 cm<sup>3</sup> min<sup>-1</sup>) atmosphere at ambient pressure from room temperature to 1000 °C. The gases evolved were led through a heated tube into a FTIR gas cell. The FTIR gas cell and the connecting tube were kept at 220 °C. The absorption spectra were recorded in the wavenumbers interval of 4,000–400 cm<sup>-1</sup> with a resolution of 4 cm<sup>-1</sup> and 60 scans averaged. The evolved gases were identified using the FTIR reference spectra in Thermo Scientific FTIR vapour phase and gases Database, Vol. 3. Powder X-ray diffraction (XRD) analysis was carried out using a Bruker D8 Advance powder X-ray diffractometer with CuK $\alpha$  source. The spectra were recorded at the standard rate of 1.5 2 $\theta$ /min. After pressing the samples into the pellets with KBr (~1.5%), the Fourier-transform infrared (FTIR) spectra were recorded with a Perkin–Elmer FTIR Spectrum 1000 spectrometer. The scanning electron microscope (SEM) DSN 962 was used to study the surface morphology and microstructure of the obtained ceramic samples.

## Results and discussion

### Thermal analysis

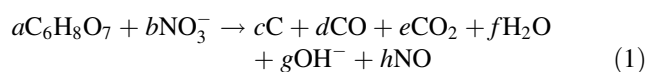
In order to explain and better understand the possible thermal decomposition behaviour of precursors and crystallization process of the sol–gel materials, the thermal analysis (TG-DTA) with simultaneous FTIR analysis of evolved gases during (FTIR-EGA) decomposition could be successfully used [22–24]. The TG-DTA curves of the YSZ nitrate–citrate gels prepared using different concentrations of ZrO(NO<sub>3</sub>)<sub>2</sub>·2H<sub>2</sub>O are displayed in Fig. 2. The impact of the initial concentration of the ZrO(NO<sub>3</sub>)<sub>2</sub>·2H<sub>2</sub>O solution is manifested in the TG–DTA curves. The decomposition process of gels can be roughly divided into three intervals. The first weight loss observed in the TG curves between room temperature and 248 °C was 38, 67 and 72% for samples 1, 2 and 3, respectively. These differences could be explained by the possible loss of some nitrate during dehydration [25] or different composition of complexes formed in gelation process due to different concentrations. In the DTA curve of sample 1 (of the lowest concentrations of ZrO(NO<sub>3</sub>)<sub>2</sub>·2H<sub>2</sub>O used in the sol–gel processing (Fig. 2), only one broad endothermic peak with top at 217 °C was observed. In the DTA curves of samples 2 and 3, additional endothermic effect with peak top at 155 °C appeared. This additional effect is complemented with the bigger mass loss at these temperatures and could be related to melting of the precursor [26] before decomposition of gel complexes.

At the second, from 250 to 330 °C, and third, from 330 to 480 °C, decomposition steps, the mass loss values of the studied samples equalized and achieved the values from 88

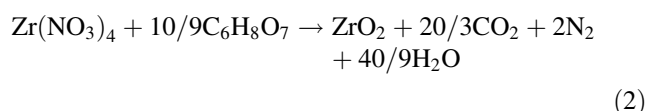
to 94 %. At these temperatures, the decomposition process was strongly exothermic (Fig. 2) with peak top at 365–370 °C characteristic for oxidation process of organic compounds.

With the temperature increase of up to 1,000 °C, the weight remains almost constant, which indicates that the decomposition and combustion of all organic components in the precursor gel were completed at below 450 °C. However, the negligible exothermic peak in the DTA curve (sample 2) at ~530 °C is also detected with a mass loss of 2%. These TG/DTA results of synthesized YSZ nitrate–citrate precursor gels show that for the preparation of bulk YSZ or thin films from Y-Zr-O nitrate–citrate sols with higher concentrations of starting materials, at least the temperature of 550 °C is needed to complete solid-state reaction.

The citrate–nitrate mixture combustion is often explained by simplified reactions with the release of CO<sub>2</sub>, H<sub>2</sub>O, CO, NO and N<sub>2</sub> [26, 27], respectively:



or



The results obtained from TG/DTA analyses complemented by FTIR/EGA permitted to understand the process more

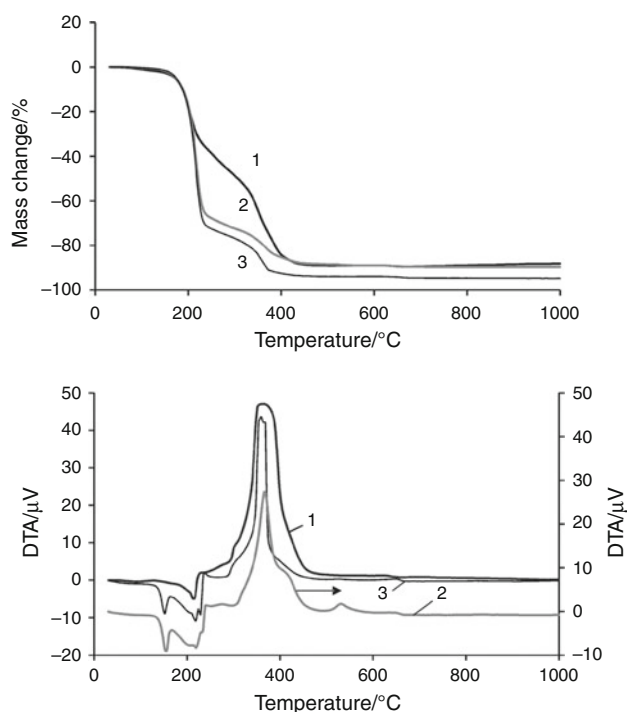


**Fig. 2** TG/DTA curves of YSZ nitrate–citrate gels having lowest concentration (sample 1), intermediate concentration (sample 2) and highest concentration (sample 3) of starting materials

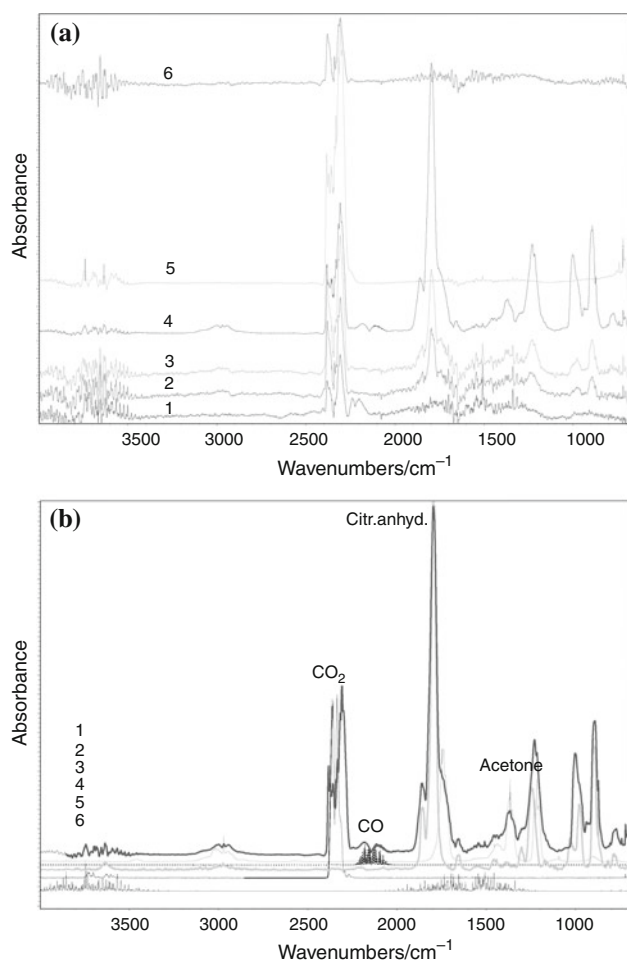


**Fig. 3** FTIR spectra of the gaseous products (EGA) of thermal decomposition of YSZ nitrate–citrate gel (sample 2) at different temperatures **a** 1 170 °C; 2 180 °C; 3 190 °C; 4 220 °C; 5 380 °C; 6 500 °C and analysis of the FTIR spectra of the evolved gas **b** 1 gases from sample 2 at 210 °C; 2 ref. acetone; 3 ref. CO; 4 ref. citraconic anhydride; 5 ref. CO<sub>2</sub>; 6 ref. H<sub>2</sub>O

deeply. At first, the composition of the evolved gases was analysed. The spectra of gases evolved at different temperatures are presented in Fig. 3. In accordance with TG curves (Fig. 2) at temperatures below 180 and above 670 °C, no remarkable gaseous products are evolved. Decomposition of the YSZ nitrate–citrate gels in the temperature region of 180–290 °C with evolution of a complex mixture of different gases was followed. For all samples, the evolution of H<sub>2</sub>O, CO<sub>2</sub>, CO, N<sub>2</sub>O, acetone, and citraconic anhydride was detected (Fig. 3a, b). Recently, the formation of citraconic anhydride was found as a result of thermal decarboxylation of citric acid in inert atmosphere [28] that supports our result of thermal decomposition of the citric complexes before oxidation.

Using the height change of characteristic peaks of the components in the evolved mixture of gases (less overlapping one's), evolution profiles of the gases were obtained (Fig. 4). Peak positions used were as follows: 3,739 cm<sup>-1</sup>

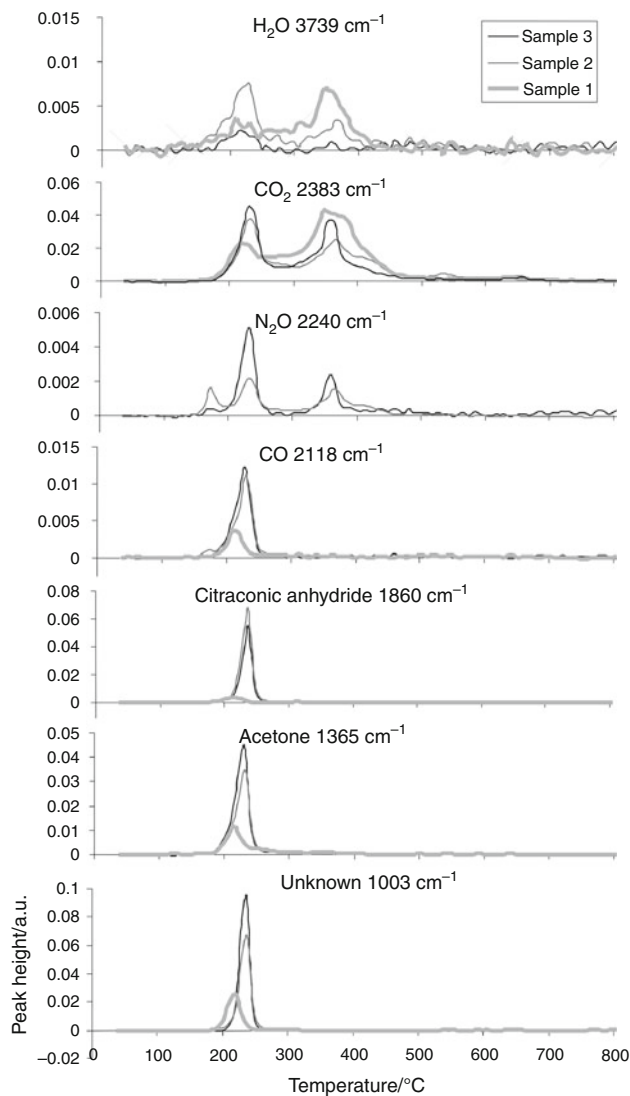


**Fig. 4** Comparison of the evolution profiles of the detected gases, samples 1–3

(O–H symmetric and asymmetric stretching vibrations) for water vapour, 2,383 cm<sup>-1</sup> (C=O asymmetric stretching vibrations) for CO<sub>2</sub>, 2,240 cm<sup>-1</sup> (O–N–N stretching vibrations) for N<sub>2</sub>O, 2,118 cm<sup>-1</sup> (C–O asymmetric stretching vibrations) for CO, 1,859 cm<sup>-1</sup> (asymmetric and symmetric coupled C=O stretching vibrations) for citraconic anhydride, 1,365 cm<sup>-1</sup> (C–O stretching vibrations) for acetone, and 1,002 cm<sup>-1</sup> for unknown component.

The endothermic decomposition reaction of gels starts with the evolution of N<sub>2</sub>O from samples 2 and 3 at about 160 °C. Species of partial decomposition of the citrate–nitrate complex together with H<sub>2</sub>O, CO<sub>2</sub>, CO and N<sub>2</sub>O are followed at 190–270 °C. In accordance with the TG results, this process is more intensive at heating samples 2 and 3. The evolution of CO, N<sub>2</sub>O, acetone, citraconic anhydride and an unknown component was essentially lower from sample 1 (Fig. 4). An exothermic combustion of intermediate

pyrolysis products with evolution of  $\text{CO}_2$  and  $\text{H}_2\text{O}$  occurs from 250 to 500 °C, more intensively from sample 1. The decomposition of the residual carbonates or burning of some residual carbon [26] is followed at temperatures above 500 °C. According to the TG/DTA/EGA results, this combustion process ends up to 750 °C.

Therefore, the concentration of the initial  $\text{ZrO}(\text{NO}_3)_2 \cdot 2\text{H}_2\text{O}$  influences the composition of the formed complexes and thereby their thermal decomposition

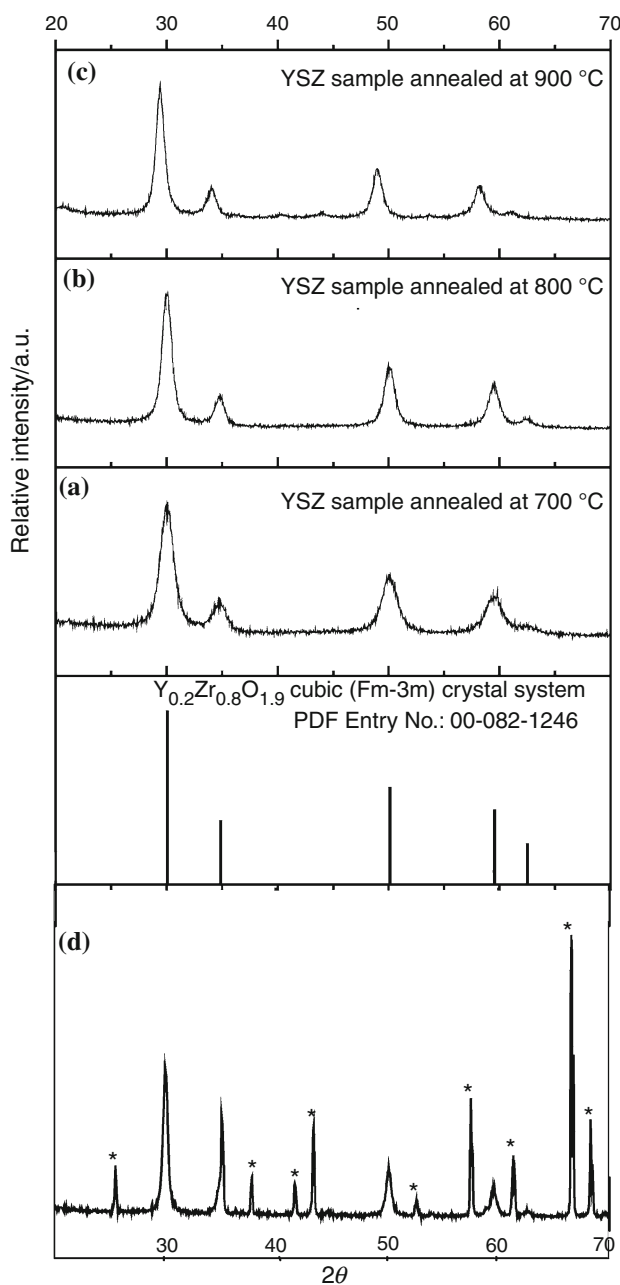


**Fig. 5** X-ray diffraction patterns of sol-gel-derived YSZ annealed from 700 to 900 °C (a, b, c) and YSZ thin film on the  $\text{Al}_2\text{O}_3$  (corundum) substrate obtained from the YSZ nitrate-citrate sol using dip-coating technique (d). \*Peaks from  $\text{Al}_2\text{O}_3$  substrate

characteristics. In case of using lower concentrations (sample 1) in gel preparation step, the evolution of partially decomposed species (citric anhydride and acetone) is less and accordingly the main decomposition occurs at higher temperatures with evolution of  $\text{CO}_2$  and water vapour.

#### X-ray diffraction

The XRD patterns of sol-gel-derived yttria-stabilized zirconia powders annealed at 700, 800 and 900 °C and YSZ thin film on the  $\text{Al}_2\text{O}_3$  substrate are shown in Fig. 5. These spectra prove that even annealing of the synthesized gel precursors at 700 °C gave  $\text{Y}_{0.2}\text{Zr}_{0.8}\text{O}_{1.9}$  compound of the cubic crystal structure (Fig. 5a). After calcination at 800 and 900 °C, the XRD pattern of YSZ powders (Fig. 5b, c) is almost identical to the previous one. XRD patterns show only small deviation of peaks width and intensity. These results are in a good agreement with the well-known tendency that at higher annealing temperatures, the crystallinity of mixed metal oxides increases. The XRD pattern of YSZ thin film obtained from YSZ nitrate-citrate sol dip-coating technique and annealed at 800 °C is shown in

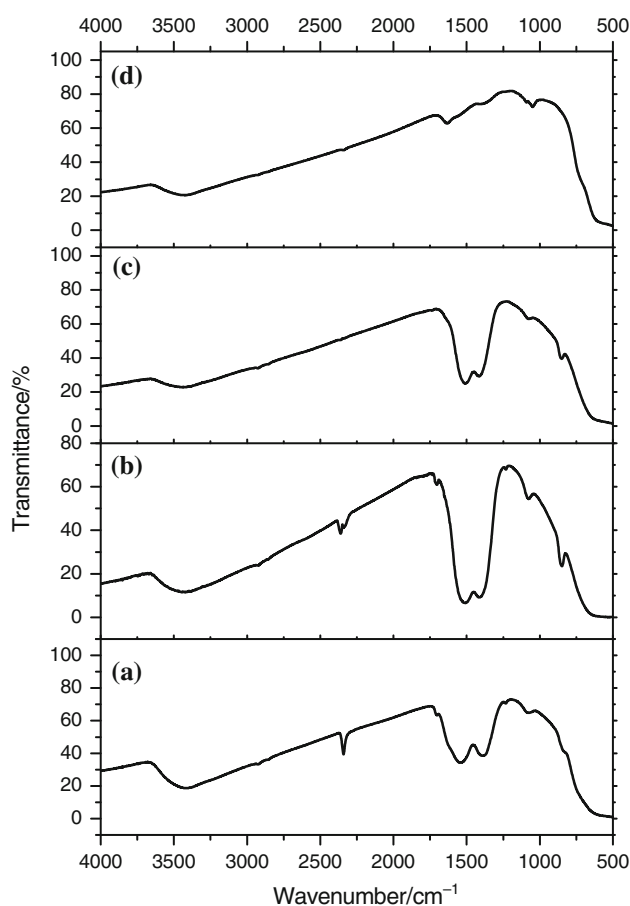


**Fig. 6** FTIR spectra of YSZ powders calcined at a 500 °C, b 700 °C, c 800 °C and d 900 °C

Fig. 5d. This XRD pattern also indicates the formation of the cubic crystal structure YSZ on the corundum surface.

#### FTIR spectroscopy

The FTIR spectra of the YSZ powders obtained from the nitrate–citrate gels at calcination in the temperature range of 500–900 °C are shown in Fig. 6. The band clearly seen in the IR spectra at  $\sim 500\text{ cm}^{-1}$  is fundamental infrared frequency attributable to the cubic  $\text{ZrO}_2$  crystal phase [29]. The broad band in the  $3,500\text{ cm}^{-1}$  region may result from atmospheric moisture retained by the KBr pellet used in the measurement or from H–O characteristic vibrations from the water adsorbed by the final products during exposure in atmosphere. A sharp small peak at  $2,345\text{ cm}^{-1}$  is attributed to the vibrational stretching of the C=O band, which is assigned to the  $\text{CO}_2$  molecules from air. For the samples heated at 500–800 °C, the two bands in the  $1,200\text{--}1,700\text{ cm}^{-1}$  region with maximum values at approximately  $1,540$  and  $1,400\text{ cm}^{-1}$  could be attributed to the ionic carbonate or oxycarbonate groups [30] in accordance with the FTIR spectrum of the YSZ sample which was annealed at 900 °C and does not contain characteristic vibrational bands in the  $1,200\text{--}1,700\text{ cm}^{-1}$  region.

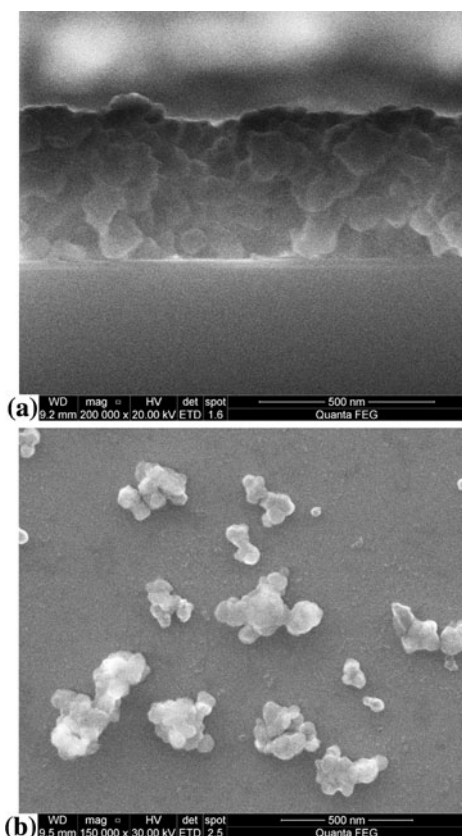


**Fig. 7** SEM micrographs of the YSZ thin film cross-section on  $\text{Al}_2\text{O}_3$  (corundum) substrate (a) and YSZ bulk powders (b), both annealed at 800 °C

#### SEM measurements

Figure 7 shows the SEM images of the yttria-stabilized zirconia thin film cross-section deposited from YSZ nitrate–citrate sol on the  $\text{Al}_2\text{O}_3$  (corundum) substrate using dip-coating technique (Fig. 7a) and YSZ powders (Fig. 7b) obtained from YSZ nitrate–citrate gel after annealing both samples at 800 °C. These SEM images demonstrate that almost spherical YSZ particles 30–70 nm in size those tend to agglomerate to 100–150-nm crystallites have formed. The aggregation of YSZ nanoparticles has caused the formation of porous materials. Thin coating of about 500 nm is obtained after 30 immersion and annealing procedures as shown in Fig. 7a.

#### Conclusions

In conclusion, the simple, inexpensive and environmentally benign aqueous sol–gel synthesis methods have been developed for the preparation of yttria-stabilized zirconia (YSZ) bulk powders and thin films on the corundum ( $\text{Al}_2\text{O}_3$ ) substrate using dip-coating technique. Regardless the impact of concentration of the  $\text{ZrO}(\text{NO}_3)_2 \cdot 2\text{H}_2\text{O}$  on the composition of the formed complexes and thereby their thermal decomposition characteristics, particularly on the composition of the evolved gases, it has insignificant effect on the YSZ powders or thin films characteristics obtained after annealing. Monophasic YSZ particles 30–70 nm in size those tend to agglomerate to 100–150-nm crystallites of cubic crystal structure were obtained at 800 °C.

**Acknowledgements** This work was supported by a grant (No. ATE-05/2010) from the Research Council of Lithuania. The authors are very thankful to Prof. S. Tamulevicius (Kaunas University of Technology) for his helpful discussions and Dr. B. Abakeviciene (Kaunas University of Technology) for technical assistance.

#### References

1. Liu J, Barnett SA. Thin yttrium-stabilized zirconia electrolyte solid oxide fuel cells by centrifugal casting. *J Am Ceram Soc.* 2002;85:3096–8.
2. Restivo TAG, Mello-Castanho SRH. Sintering studies on Ni–Cu–YSZ SOFC anode cermet processed by mechanical alloying. *J Therm Anal Calorim.* 2009;97:775–80.
3. Diaz-Parralejo A, Ortiz AL, Caruso R. Effect of sintering on the microstructure and mechanical properties of  $\text{ZrO}(2)\text{-}3\text{ mol}\% \text{Y}(2)\text{O}(3)$  sol-gel films. *Ceram Int.* 2010;36:2281–6.
4. Lenormand P, Caravaca D, Laberty-Robert C, Ansart F. Thick films of YSZ electrolytes by dip-coating process. *J Eur Ceram Soc.* 2005;25:2643–6.
5. Gaudon M, Laberty-Robert C, Ansart F, Stevens P. Thick YSZ films prepared via a modified sol–gel route: thickness control (8–80  $\mu\text{m}$ ). *J Eur Ceram Soc.* 2006;26:3153–60.
6. Arico E, Tabuti F, Fonseca FC, de Florio DZ, Ferlauto AS. Carbothermal reduction of the YSZ–NiO solid oxide fuel cell

- anode precursor by carbon-based materials. *J Therm Anal Calorim.* 2009;97:157–61.
7. Kim SG, Nam SW, Yoon SP, Hyun SH, Han J, Lim TH, Hong SA. Sol-gel processing of yttria-stabilized zirconia films derived from the zirconium *n*-butoxide-acetic acid-nitric acid-water-isopropanol system. *J Mater Sci.* 2004;39:2683–8.
  8. Xu X, Xia C, Huang S, Peng D. YSZ thin films deposited by spin-coating for IT-SOFCs. *Ceram Int.* 2005;31:1061–4.
  9. Dell'Agli G, Mascolo G, Mascolo MC, Pagliuca C. Microwave-hydrothermal treatment of mechanical mixtures of ZrO<sub>2</sub> xerogel and crystalline Y<sub>2</sub>O<sub>3</sub>. *J Therm Anal Calorim.* 2005;80:721–5.
  10. Miyazaki H. The effect of TiO<sub>2</sub> additives on the structural stability and thermal properties of yttria fully-stabilized zirconia. *J Therm Anal Calorim.* 2009;98:343–6.
  11. Morales M, Roa JJ, Capdevila XG, Segarra M, Pinol S. Mechanical properties at the nanometer scale of GDC and YSZ used as electrolytes for solid oxide fuel cells. *Acta Mater.* 2010;58:2504–9.
  12. Diaz-Parralejo A, Ortiz AL, Rodriguez-Rojas F, Guiberteau F. Effect of N<sub>2</sub> sintering atmosphere on the hardness of sol-gel films of 3 mol% Y<sub>2</sub>O<sub>3</sub>-stabilized ZrO<sub>2</sub>. *Thin Solid Films.* 2010;518:2779–82.
  13. Amezcaga-Madrid P, Antunez-Flores W, Gonzalez-Hernandez J, Saenz-Hernandez J, Campos-Venegas K, Solis-Canto O, Ornelas-Gutierrez C, Vega-Becerra O, Martinez-Sanchez R, Miki-Yoshida M. Microstructural properties of multi-nano-layered YSZ thin films. *J Alloys Compd.* 2010;495:629–33.
  14. Diaz-Parralejo A, Ortiz AL, Caruso R, Guiberteau F. Effect of type of solvent alcohol and its molar proportion on the drying critical thickness of ZrO<sub>2</sub>-3 mol% Y<sub>2</sub>O<sub>3</sub> films prepared by the sol-gel method. *Surf Coat Technol.* 2011;205:3540–5.
  15. Diaz-Parralejo A, Macias-Garcia A, Sanchez-Gonzalez J, Diaz-Diez MA, Cuerda-Correa EM. A novel strategy for the preparation of yttria-stabilized zirconia powders. Deposition and scratching of thin obtained by the sol-gel method. *J Non-Cryst Solids.* 2011;357:1090–5.
  16. Cheng J, Bao W, Han C, Cao W. A novel electrolyte for intermediate solid oxide fuel cells. *J Power Sources.* 2010;195:1849–53.
  17. Cushing BL, Kolesnichenko VL, O'Connor CJ. Recent advances in the liquid-phase syntheses of inorganic nanoparticles. *Chem Rev.* 2004;104:3893–946.
  18. Katelnikovas A, Barkauskas J, Ivanauskas F, Beganskiene A, Kareiva A. Aqueous sol-gel synthesis route for the preparation of YAG: evaluation of sol-gel process by mathematical regression model. *J Sol-Gel Sci Technol.* 2007;41:193–201.
  19. Mackenzie JD, Bescher EP. Chemical routes in the synthesis of nanomaterials using the sol-gel process. *Accounts Chem Res.* 2007;40:810–8.
  20. Egger P, Soraru GD, Dire S. Sol-gel synthesis of polymer-YSZ hybrid materials for SOFC technology. *J Eur Ceram Soc.* 2004;24:1371–4.
  21. Zalga A, Abakeviciene B, Zarkov A, Beganskiene A, Kareiva A, Tamulevicius S. On the properties of yttria-stabilized zirconia thin films prepared by sol-gel method. *Mater Sci (Medžiagotyra).* 2011;17:191–6.
  22. Miller TW. Use of TG/FT-IR in material characterization. *J Therm Anal Calorim.* 2011;106:249–54.
  23. Acik IO, Madarasz J, Krunks M, Tönsuaadu K, Pokol G, Niinistö L. Titanium(IV) acetylacetonate xerogels for processing titania films. *J Therm Anal Calorim.* 2009;97:39–45.
  24. Otto K, Acik IO, Tönsuaadu K, Mere A, Krunks M. Thermoanalytical study of precursors for In<sub>2</sub>S<sub>3</sub> thin films deposited by spray pyrolysis. *J Therm Anal Calorim.* 2011;105:615–23.
  25. Marinšek M, Gomilšek JP, Arčon I, Čeh M, Kodre A, Maček J. Structure development of NiO-YSZ oxide mixtures in simulated citrate-nitrate combustion synthesis. *J Am Ceram Soc.* 2007;90:3274–81.
  26. Marinšek M, Zupan K, Maček J. Citrate-nitrate gel transformation behavior during the synthesis of combustion-derived NiO-yttria-stabilized zirconia composite. *J Mater Res.* 2003;18:1551–60.
  27. Banerjee S, Kumar A, Devi PS. Preparation of nanoparticles of oxides by the citrate-nitrate process. Effect of metal ions on the thermal decomposition characteristics. *J Therm Anal Calorim.* 2011;104:859–67.
  28. Wyrzykowski D, Hebanowska E, Nowak-Wicz G, Makowski M, Chmurzyn'ski L. Thermal behaviour of citric acid and isomeric aconitic acids. *J Therm Anal Calorim.* 2011;104:731–5.
  29. Phillippi CM, Mazdiyasi KS. Infrared and Raman spectra of zirconia polymorphs. *J Am Ceram Soc.* 1971;54:254–8.
  30. Chroma M, Pinkas J, Pakutinskiene I, Beganskiene A, Kareiva A. Processing and characterization of sol-gel fabricated mixed metal aluminates. *Ceram Int.* 2005;31:1123–30.